

B1+ inhomogeneity compensated MRF using simultaneous AFI

Taehwa Hong¹, Min-Oh Kim¹, Dongyeob Han¹, Dosik Hwang¹, and Dong-Hyun Kim¹
¹Electrical & Electronic Engineering, Yonsei University, Seodamun-gu, Seoul, Korea

Target audience: Researchers who are interested in multi contrast quantification.

Purpose: MR fingerprinting (MRF)¹ is a rapid method for quantification of multiple properties of tissues (T_1 , T_2 and M_0). The technique however can be hampered by B1 inhomogeneity at high field strengths (3T or above). In a previous MRF study², a correction method using separately acquired B1⁺ map was introduced to improve MRF quantification accuracy. Here, MRF combined with actual flip angle (AFI)³ technique is proposed to achieve simultaneous B1⁺ mapping and B1⁺ map compensated MRF.

Methods: An AFI scheme is adapted to the inversion-recovery balanced steady state free-precession based MRF sequence. Fig. 1 shows a sequence diagram. Identical flip angles and TRs for the first two measurements ($FA_1=FA_2$, $TR_1=TR_2$) were applied and the transverse magnetization was spoiled at the end of the TR_1 . The signal equation can be modeled as Eq. 1 and 2. From this, the actual flip angle can be derived as Eq. 3. If T_1 relaxation effect is negligible during first two TRs, the estimated flip angle can be derived as the ratio of two signals (Eq. 4). Once the estimated flip angle is calculated, B1⁺ map can be obtained by dividing estimated flip angle by nominal flip angle (Eq. 5).

$$S_1 = |M_0 \sin(\alpha) \exp(-\frac{TE}{T_2})| \quad (1), \quad S_2 = |M_0 \{1 - (\cos(\alpha) + 1) \exp(-\frac{TR}{T_1})\} \sin(\alpha) \exp(-\frac{TE}{T_2})| \quad (2)$$

$$\alpha = \cos^{-1} \left(\frac{S_2 + 1}{S_1} \right) \quad (3), \quad \alpha_{est} \approx \cos^{-1} \left(\frac{S_2}{S_1} \right), \text{ where } \alpha < 90^\circ \quad (4), \quad B1^{+}_{normalized} = \frac{\alpha_{est}}{\alpha_{nominal}} \quad (5)$$

This approximation causes an estimation error in B1⁺ map and we analyzed this modeling error as a function of TR (3:0.1:10ms), T_1 (100:5:3000ms) and actual flip angle (15:1:80°) by simulation.

To estimate the flip angle and the B1⁺ map, the first two measurements images were reconstructed from low frequency region k-space data (16x16) to reduce the undersampling artifact. For each voxel, T_1 and T_2 maps were obtained by matching using a dictionary generated by including B1⁺ measurements as known information. 500 undersampled images were acquired with radial trajectory (acceleration factor: 16) with a range of FA (0~80°, $FA_1=FA_2=45^\circ$) and TR (5~8ms, $TR_1=TR_2=5$ ms) in 64s; FOV=256x256mm; in-plane resolution=2x2mm²; slice thickness=5mm. All experiments were performed in *in-vivo* human brain on a 3T scanner. In addition, to compare with the conventional B1⁺ mapping, double angle method (DAM)⁴, two GRE images were acquired with FA = 30°, 60°, TR/TE = 5000/5ms, and the same RF profile with the proposed sequence was used to make the slice profile condition identical⁵. Other scan parameters were same as the MRF experiment.

Results and Discussion: The relative estimation error due to ignoring T_1 relaxation effect (Eq. 4) is presented in Fig. 2. Fig. 2(a) shows the relative estimation error dependency to actual flip angle when TR=5ms and $T_1=1000$ ms. Fig. 2(b) shows a simulated relative estimation error map at $\alpha=45^\circ$. The error decreases with T_1 and increases with TR leading to overestimation in B1⁺ mapping. Fig. 3(a-b) show obtained B1⁺ map from the proposed method and the conventional DAM respectively. DAM B1⁺ map was fitted with 6th order polynomial to reduce the error at CSF region. Fig. 3c shows a line profile of each method. The proposed method shows an underestimated result. We used short RF pulse duration in order to achieve fast imaging, which resulted in slice profile imperfection. Thus, this factor can lead to B1⁺ map underestimation⁵. An improved RF pulse (with increased time-bandwidth product) should alleviate this underestimation. MRF T_1 map with and without B1⁺ correction are shown in Fig. 4(a-b), and T_2 map, Fig. 4(d-e). Corrected T_1 and T_2 maps show improved contrast between gray and white regions and also improved homogeneity in gray and white matters. Fig. 4(c) and (f) show the normalized difference between before and after correction of each T_1 and T_2 map. The normalized difference maps show pattern similar to B1⁺ pattern. Especially, the applied B1⁺ correction affects more on T_2 estimation than T_1 estimation which is in agreement with the previous study².

Conclusion: A simultaneous B1⁺ mapping with multiple tissue parameters was demonstrated in this study. This B1⁺ map can be used to increase the accuracy in parameter mapping.

Acknowledgement: This work was supported by Samsung Electronics.

References: [1] Dan Ma et al., Nature, 495:187-192, 2013. [2] Yong Chen et al., ISMRM, 0561, 2014. [3] Vasily L. Yarnykh., MRM, 57:192-200, 2007. [4] Charles H. Cunningham, et al., MRM, 55:1326-1333, 2006. [5] Jinghua Wang et al., MRM, 56:463-468, 2006.

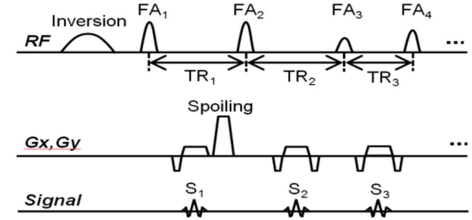


Fig. 1. Pulse sequence diagram. Identical FAs and TRs were applied for the first two measurements. The transverse magnetization was spoiled at the end of TR_1 .

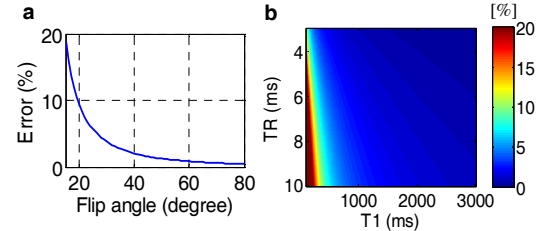


Fig. 2. (a) Relative estimation error dependency to actual flip angle at TR=5ms and $T_1=1000$ ms. (b) Simulated relative estimation error map due to ignoring T_1 relaxation effect.

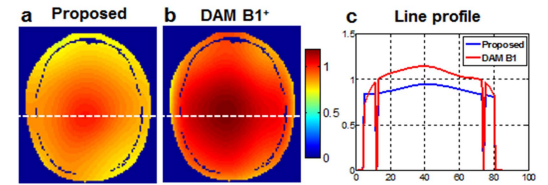


Fig. 3. Obtained B1⁺ map from (a) proposed method, and (b) DAM. DAM B1⁺ map was fitted with 6th order polynomial.

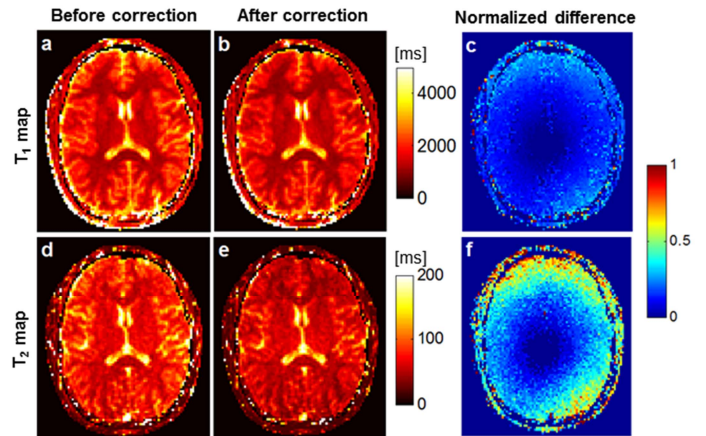


Fig. 4. Obtained T_1 and T_2 map with and without B1⁺ correction. (a-b) T_1 map before and after correction are in the upper row. (d-e) T_2 map before and after correction are in the lower row. (c, f) The difference maps were normalized by corrected map as following: $[\text{uncorrected}-\text{corrected}]/\text{corrected}$.